

Multi-spectral Class Center Network for Face Manipulation Detection and Localization

Changtao Miao¹, Qi Chu¹, Zhentao Tan^{1,2}, Zhenchao Jin³, Wanyi Zhuang¹,
Yue Wu², Bin Liu¹, Honggang Hu¹, Nenghai Yu¹

¹University of Science and Technology of China ²DAMO Academy, Alibaba Group

³The University of Hong Kong

Abstract

As Deepfake content continues to proliferate on the internet, advancing face manipulation forensics has become a pressing issue. To combat this emerging threat, previous methods mainly focus on studying how to distinguish authentic and manipulated face images. Although impressive, image-level classification lacks explainability and is limited to certain specific application scenarios, which spawns recent research on pixel-level prediction for face manipulation forensics. However, existing forgery localization methods suffer from imprecise and inconsistent pixel-level annotations. To alleviate these problems, this paper first re-constructs the FaceForensics++ dataset by introducing pixel-level annotations, then establishes an comprehensive benchmark for localizing tampered regions. Besides, a novel **Multi-Spectral Class Center Network (MSCCNet)** is proposed for face manipulation detection and localization. Specifically, inspired by the power of frequency-related forgery traces, we design a **Multi-Spectral Class Center (MSCC)** module to learn more generalizable and semantic-agnostic features. Based on the features of different frequency bands, the MSCC module collects multi-spectral class centers and computes pixel-to-class relations. Applying multi-spectral class-level representations suppresses the semantic information of the visual concepts which is insensitive to manipulated regions of forgery images. Furthermore, we propose a **Multi-level Features Aggregation (MFA)** module to employ more low-level forgery artifacts and structural textures. Experimental results quantitatively and qualitatively demonstrate the effectiveness and superiority of the proposed MSCCNet on comprehensive localization benchmarks. We expect this work to inspire more studies on pixel-level face manipulation localization. *The annotations and codes are available.*

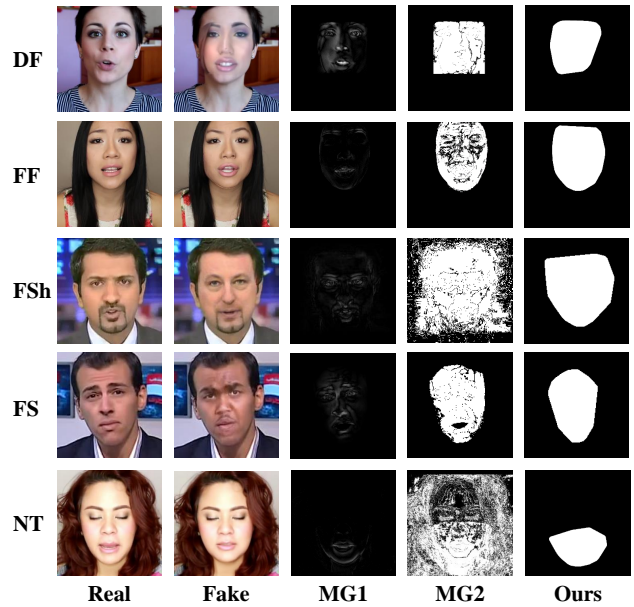


Figure 1. The different pixel-level annotation methods for FaceForensics++ (FF++) [51]. DF [13], FF [59], FSh [32], FS [17], and NT [58] rows are five different Deepfake technologies. The Real and Fake columns depict authentic and corresponding manipulated faces, respectively. In contrast, the MG1 column exhibits dispersed points, whereas the MG2 column contains numerous background regions. This paper proposes an annotation method (Ours column) that yields more precise and comprehensive masks of the tampered regions.

1. Introduction

Continuous advancements in Deepfake technologies [13, 17, 32, 58, 59] are resulting in the creation of remarkably realistic images and videos, exhibiting fewer noticeable tampering artifacts. Despite their applications in the film and entertainment industries, these Deepfake tools are also exploited for malicious purposes such as creating political propaganda or pornographic content. To address public

concerns regarding misinformation, face manipulation detectors [4, 9, 19, 33–35, 35, 39, 48, 53, 61, 69, 70, 75, 76] which aim to provide coarse-grained binary classification results (real or fake) at the image-level or video-level have geared extensive attentions. While the pixel-level localization of manipulated regions of Deepfake images, which has a pivotal role in analyzing and explaining the Deepfake detection results, receives inadequate attention.

One obstacle in the development of pixel-level face manipulation localization technology is the scarcity of publicly available datasets featuring pixel-level annotations. To cope with the problem, some recent works [12, 25, 26, 28, 45, 56, 65] proposed their algorithms to extract pixel-level annotations from existing face manipulation datasets (e.g., FaceForensics++ [51]). Despite impressive, it is difficult to compare their designed pixel-level face manipulation localization frameworks with each other due to the diverse pixel-level annotations they employ. Besides, the quality of their annotation is unsatisfactory. There are two prevalent approaches for acquiring pixel-level annotations, denoted as *MG1* and *MG2* in Figure 1. *MG1* is used in some studies [9, 25, 33], which computes the pixel-wise difference between fake image and corresponding real image in RGB channels, converts it into grayscale, and divides by 255 to produce a map within the range of [0, 1]. Some other works [12, 61] adopt *MG2* that binarizes the output of *MG1* using a pre-defined threshold to obtain a binary mask for manipulation regions. As shown in Figure 1, the annotations from *MG1* are incomplete while those from *MG2* contain authentic background regions. For example, the NeuralTextures (NT) [58] only manipulates local areas of expression (e.g., mouth, nose, etc.) as shown in the last row, but both two annotations contain errors. Such imprecise and inconsistent annotations greatly hinder the advancement of face manipulation localization.

To address this problem, we adopt a sequence of image processing operations to compensate for the deficiency of pixel-level manipulation mask annotations in the FF++ [51] dataset. As illustrated in the last column of Figure 1, the proposed annotation strategy yields a more rational manipulated region mask that conforms to the technical characteristics of different face manipulation technologies (e.g., NT [58]). Leveraging the FF++ benchmark dataset with the extracted pixel-level annotations, we further establish a comprehensive benchmark for face manipulation localization. Specifically, we reproduce several existing forgery localization-related methods using their publicly available source codes in our benchmark, including: 1) Face manipulation detection methods with segmentation loss [7, 61]. 2) Face manipulation localization methods [12, 45]. 3) Image forgery localization methods [10, 22, 30, 31]. While, extensive experimental results of our benchmark suggest that existing forgery localization methods are far from satisfactory,

which motivates us to develop a more effective framework for face manipulation localization.

Among them, earlier work [12] attempts to take advantage of the attention maps to generate forged regions rather than specialized localization branches, which misses rich global contextual information. Later approaches [7, 25, 26, 28, 45, 56, 61, 65] widely employ the pipeline of semantic segmentation since the simple decoder network and segmentation loss can naturally support the face manipulation localization task, which learn the discriminative global context features and obtain more precise localization results. Nevertheless, directly applying the segmentation framework to the forgery localization task may not be optimal, as the semantic segmentation models focus on the semantic objective information while the face manipulation localization model needs to predict tampering locations exclusively [3, 66, 77]. Some studies [10, 23] also show that the deep semantic objective information would impact the learning of tampered features.

In order to inhibit the semantic object content in the deeper localization branch, we propose a novel **Multi-Spectral Class Center Network** (MSCCNet) for face manipulation detection and localization, which exploits class-level representations of different frequency component features to enhance the tamper localization capability. The MSCCNet consists of two key components: **Multi-level Features Aggregation** (MFA) and **Multi-Spectral Class Center** (MSCC) modules. The proposed MFA module effectively aggregates the low-level texture information and forgery artifacts, as these cues are predominantly present in shallow features [37, 39]. The MSCC module is designed to extract the semantic-agnostic forgery features by suppressing the semantic objective representation capability of the network. Specifically, we first decompose the semantic features using a frequency transformation and calculate pixel-class relations within each spectral feature. Then, the weighted attention of different frequency bands is acquired by computing similarity maps between different spectral class centers and the corresponding partial semantic features. Finally, we employ weighted attention to alleviate the impact of semantic objective information and refine the original global context. Meanwhile, in the image forgery localization community, some researchers [10, 22, 23, 30] exploit the noise or frequency information to suppress image semantic content, but they normally extract noise or frequency maps on input RGB images. In this way, the deeper-layer features may remain semantic-aware and consequently cannot preserve semantic-agnostic capability at the localization decoder network. In contrast, our MSCC module first attempts to mitigate this phenomenon in the localization decoder network, and achieves satisfactory results.

In a nutshell, our main contributions could be summa-

rized as:

- To facilitate the localization tasks, we first reconstruct the FaceForensics++ (FF++) datasets by introducing more rational pixel-level annotations. Then we conduct a comprehensive benchmark for face manipulation localization based on the annotated FF++ datasets.
- A novel Multi-spectral Class Center Network (MSCCNet) is designed for face manipulation localization, which consists of a Multi-level Features Aggregation (MFA) module and a Multi-spectral Class Center (MSCC) module for learning more generalizable and semantic-agnostic features.
- Extensive experiments on pixel-level FF++ datasets show that MSCCNet compares favorably against the benchmark methods.

2. Related Work

2.1. Face Manipulation Detection and Localization

Early face manipulation detection methods [6, 11, 18, 19, 46, 47] utilize intrinsic statistics or hand-crafted features to model spatial manipulation patterns. Recently, data-derived detection models utilize spatial artifacts [1, 54, 55, 57, 60, 62, 75, 79, 80] to learn discriminative features and achieve remarkable detection performance. However, these methods ignore the importance of the manipulated regions for face manipulation detection. Some other studies [9, 33, 42, 53, 61, 70, 76] explore the spatially tampered regions as additional supervised signals with segmentation loss to improve the performance of real-fake binary classification, while they do not make prediction and evaluation for manipulated regions.

Recently, a few methods [12, 25, 26, 28, 45, 56, 65] have superficially examined the positioning problem and there are still many deficiencies. For example, FFD [12] directly applies the low-resolution attention map of the network to detect the tampered regions in face manipulation images, but it lacks global context information. To address this issue, some face manipulation localization methods [25, 26, 28, 45, 56] employ a semantic segmentation pipeline to segment the fake regions. Specifically, Multi-task [45] designs an additional segmentation branch for localizing manipulated regions. The prior arts [25, 56] present a localization method for GAN-synthesized fake images, and yet they cannot be accommodated to face manipulation data. But semantic segmentation networks are adept at learning semantic dependent objects, in other words, they cannot adapt well to tampering target localization [3, 77]. Because the manipulated regions (or objects) are semantic-agnostic features, compressing image content information is the key to developing face manipulation locators within

the image semantic segmentation network. In this paper, we proposed a multi-spectral class center module to enhance the forgery region localization ability of the localization branch and suppress the semantic objective information in images.

2.2. Image Forgery Detection and Localization

Image forgery technologies (*e.g.*, splicing, copy-move, removal) have been around for a long time in contrast to the recent rise of face manipulation methods. Image forensics tasks also aim to detect images as spoof or bona fide and locate the tampering regions, but most image forgery localization methods [3, 23, 31, 77] only focus on fake image datasets rather than real-fake mixed datasets. One type of localization method is to segment the entire input image [23, 66], and the other type is to perform binary classification repeatedly using a sliding window [50]. Our MSCCNet framework takes the cropped facial areas as the input, which reduces the computational expenses compared to the full-image input and sliding window approaches. Image forgery localization tasks also appear to be a simplified case of image semantic segmentation and thus they likewise confront the perturbation of semantic objective content. In addition, image forgery localization methods [10, 30, 31] have only been studied for traditional image tampering techniques and cannot be tailored to the latest face manipulation algorithms. In this paper, we mainly focus on localizing the manipulated regions created by advanced face forgery techniques [13, 17, 32, 58, 59].

2.3. Noise and Frequency Forgery Clues

To learn semantic-agnostic features, many image forgery localization approaches [10] exploit noise or frequency artifacts to inhibit image content. MVSS [10] adopts the BayarConv [5] to extract the noise-view patterns on the input RGB image and then build a noise-sensitive branch. CAT-Net [30] focuses on JPEG compression artifacts and uses a segmentation model based on DCT coefficients. HiFi-Net [22] extracts features of the given input RGB image via the color and frequency modules, and this frequency module consists of a Laplacian of Gaussian (LoG). The deep features of prior methods [10, 22, 30] are a risk that they may retain semantic-related information. In the face manipulation detection community, most methods [9, 16, 21, 37, 39, 48] also extract frequency- or noise-related artifacts from the input RGB image. Other studies [41, 43, 44] learn frequency forgery traces to detect manipulated face images, range from shallow layer [41] or multi-layers [43, 44]. However, they are only focusing on face manipulation detection tasks rather than localization tasks. In a nutshell, none of the prior arts suppress semantic content features in the deeper localization branch. Instead, we propose a multi-spectral class center module in the decoder to learn semantic-agnostic fea-

tures.

2.4. Semantic Segmentation

Semantic segmentation tasks aim to generate pixel-wise semantic object predictions (segmentation masks) for a given image [8, 27, 38, 52, 67, 71, 72, 74]. The face manipulation localization and semantic segmentation are very similar, differing only in the object type and class (*i.e.*, manipulated and authentic). Hence, the existing image forgery localization [10, 22, 23, 30, 31, 66] and current face manipulation localization methods [25, 26, 45, 56] employ a semantic segmentation pipeline [8, 52] to segment the fake regions. However, early methods [8, 52, 67, 74] still do not sufficiently explore global contextual information. Subsequent semantic segmentation researches [27, 38, 71, 72] learn more discriminative global contextual features, but since they are not specifically designed for the localization task, there remain issues with interference from semantic objective information. In this paper, we proposed MSCCNet to suppress the semantic objective information in global contextual features.

3. Methodology

3.1. Problem Formulation

As demonstrated in Figure 2 (a), our proposed face manipulation forensics architecture consists of a backbone network, a classification branch, and a localization branch, where the backbone network is utilized to project each input image $\mathcal{I} \in \mathbb{R}^{3 \times H \times W}$ into multi-scale feature space $\mathcal{F} = \{\mathcal{F}_1, \mathcal{F}_2, \mathcal{F}_3\}$, where $H \times W$ is the shape of the input image. After that, a multi-level forgery patterns aggregation scheme is designed to aggregate \mathcal{F} and output $\mathcal{F}_A \in \mathbb{R}^{C \times h \times w}$, where C denotes for the number of feature channels.

Next, to exploit the global contextual representation of tampered regions over different frequency bands from aggregated \mathcal{F}_A , we propose the multi-spectral class center (MSCC) module as \mathcal{M} , and then we have:

$$\mathcal{F}_M = \mathcal{M}(\mathcal{F}_A), \quad (1)$$

where $\mathcal{F}_M \in \mathbb{R}^{C \times h \times w}$ is the enhanced features from the perspective of centers of different spectral classes. Finally, \mathcal{F}_M is leveraged to predict the label of each pixel in the input image:

$$\mathcal{P}_1 = \text{Upsample}_{8 \times}(\mathcal{C}_1(\mathcal{F}_M)), \quad (2)$$

where \mathcal{C}_1 is a pixel-level classification head and $\mathcal{P}_1 \in \mathbb{R}^{k \times H \times W}$ indicates the predicted pixel-level class probability distribution. Moreover, we apply the last layer output features \mathcal{F}_3 of the backbone network as image-level classification head \mathcal{C}_2 input, we have:

$$\mathcal{P}_2 = \mathcal{C}_2(\mathcal{F}_3), \quad (3)$$

in which, $\mathcal{P}_2 \in \mathbb{R}^k$ represents the image-level prediction probability distribution. Here, k is the number of classes and $k = 2$.

3.2. Multi-level Features Aggregation

The forgery artifacts (*e.g.*, blending boundary, check-board, blur artifacts, etc.) and local structure are low-level texture features, which are mostly exiting shallow layers of the network [37, 39]. However, previous face manipulation localization methods [12, 45] primarily focused on deep semantic information and disregarded low-level texture features and location information, which would result in coarse and inaccurate output and disrupt some crucial low-level details (see Figure 4). To leverage the forgery-related low-level texture features, we propose the Multi-level Features Aggregation (MFA) scheme, which exploits texture-related information from multi-level and enhances the texture details of high-level semantic features.

As shown in Figure 2 (b), we first gain multi-level features $\mathcal{F}_1, \mathcal{F}_2, \mathcal{F}_3$ from the backbone network and then employ three different aligned layers (*i.e.*, $\mathcal{N}_1, \mathcal{N}_2$, and \mathcal{N}_3) for each of them:

$$\mathcal{F}'_1 = \mathcal{N}_1(\mathcal{F}_1), \mathcal{F}'_2 = \mathcal{N}_2(\mathcal{F}_2), \mathcal{F}'_3 = \mathcal{N}_3(\mathcal{F}_3), \quad (4)$$

where $\mathcal{F}'_1, \mathcal{F}'_2, \mathcal{F}'_3 \in \mathbb{R}^{C \times h \times w}$. Each aligned layer consists of a *Conv* and a *Downsample*, which aligns the different level features to assure the effectiveness of the lower-level texture information. Then, we aggregate the aligned multi-level features $\mathcal{F}'_1, \mathcal{F}'_2, \mathcal{F}'_3$ by channel-wise concatenation operation *Cat* as follows:

$$\mathcal{F}_A = \text{Conv}(\text{Cat}([\mathcal{F}'_1, \mathcal{F}'_2, \mathcal{F}'_3])). \quad (5)$$

where $\mathcal{F}_A \in \mathbb{R}^{C \times h \times w}$ and the *Conv* layer to make the channel size of $3C$ to C .

3.3. Multi-spectral Class Center

Previous face or image manipulation localization approaches [10, 25, 26, 45, 56, 65] apply semantic segmentation pipeline for localization decoder network since the discriminative contextual features play a crucial role in predicting meaningful object regions. However, these off-the-shelf semantic segmentation networks [8, 27, 38, 52, 67, 71, 72, 74] are not suitable for face manipulation localization tasks [3, 77]. As face manipulation localization models solely require the localization of tampered regions rather than all meaningful regions, further analysis indicates that semantic objective features interfere with the forgery cue [10, 23]. Therefore, the primary concern is how to develop and train a face manipulation localization model that can acquire semantic-agnostic features with sensitivity towards manipulations. The manipulated elements have discrepancies in the frequency domain compared to the authentic

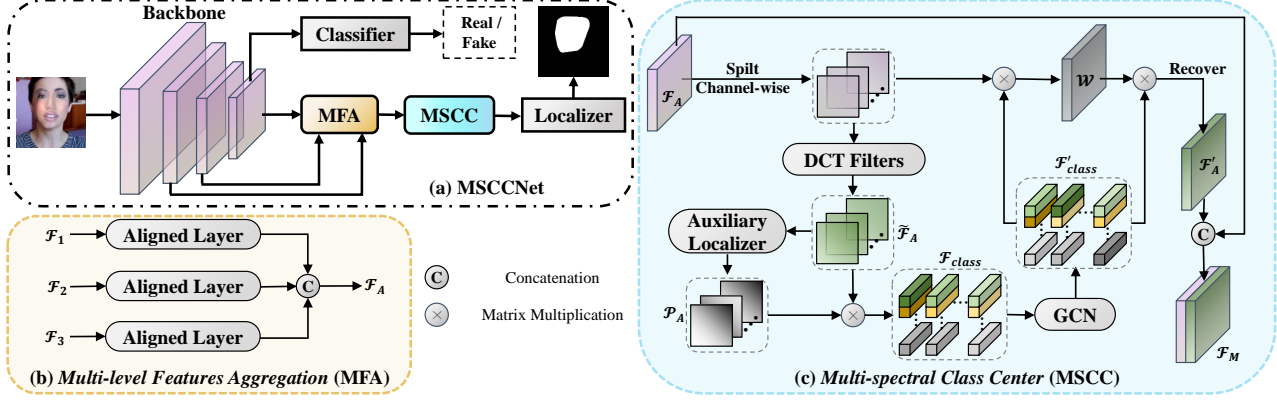


Figure 2. Detailed architecture of the proposed MSCCNet. The overall network structure is shown in (a), which consists of a backbone network, a classification branch, and a localization branch. (b) shows the scheme of the forgery-related low-level texture features aggregation. (c) illustrates the process of multi-spectral class centers and different frequency attention calculations. They are solely dedicated to enhancing the capabilities of the localization branch.

part, and extracting frequency information in the contextual features helps to suppress the semantic objective features [9, 37, 39, 48]. Inspired by these motivations, we propose a novel Multi-spectral Class Center (MSCC) module to learn semantic-agnostic forgery features from the different-frequency bands perspective, as shown in Figure 2 (c).

3.3.1 Discrete Cosine Transform Filters

Following [2, 49], the 2D Discrete Cosine Transform (DCT) filters basis functions as follows:

$$D_{u,v} = \sum_{i=0}^{H-1} \sum_{j=0}^{W-1} d_{i,j} \cos\left(\frac{\pi u}{U}\left(i + \frac{1}{2}\right)\right) \cos\left(\frac{\pi v}{V}\left(j + \frac{1}{2}\right)\right) \\ \text{s.t. } u \in \{0, 1, \dots, U-1\}, v \in \{0, 1, \dots, V-1\}, \quad (6)$$

where $d \in \mathbb{R}^{H \times W}$ is a two-dimensional data and $D_{u,v} \in \mathbb{R}^{H \times W}$ is the 2D DCT frequency spectrum with the transformation basis of (u, v) . For simplicity, we define the above DCT operation as $\mathcal{D}_n(\cdot)$, in which $n \in \{0, 1, \dots, N-1\}$ and N is the number of frequency transformation basis of (u, v) . In this paper, we first split the features $\mathcal{F}_A \in \mathbb{R}^{C \times h \times w}$ into N parts along the channel dimension, where each channel of the n -th part feature $\mathcal{F}_A^n \in \mathbb{R}^{c \times h \times w}$ is defined $f_i^n \in \mathbb{R}^{h \times w}, i \in \{0, 1, \dots, c-1\}$ and $c = \frac{C}{N}$. Then, every f_i^n is transformed through $\mathcal{D}_n(\cdot)$ with n -th transformation basis (u, v) , as follows:

$$\tilde{\mathcal{F}}_A^n = \text{Cat}([\mathcal{D}_n(f_0^n), \mathcal{D}_n(f_1^n), \dots, \mathcal{D}_n(f_{c-1}^n)]), \quad (7)$$

where $\tilde{\mathcal{F}}_A^n \in \mathbb{R}^{c \times h \times w}$ is the frequency features for specific spectral component. Similarly, we can obtain the frequency information of the \mathcal{F}_A for all spectral components and concatenate them together channel-wise:

$$\tilde{\mathcal{F}}_A = \text{Cat}([\tilde{\mathcal{F}}_A^0, \tilde{\mathcal{F}}_A^1, \dots, \tilde{\mathcal{F}}_A^{N-1}]), \quad (8)$$

in which, $\tilde{\mathcal{F}}_A \in \mathbb{R}^{N \times c \times h \times w}$ are multi-spectral feature maps with N different frequency bands (*i.e.*, N transformation basis).

3.3.2 Multi-spectral Class Center

After getting the multi-spectral feature maps $\tilde{\mathcal{F}}_A \in \mathbb{R}^{N \times c \times h \times w}$, we calculate the coarse segmentation predictions of different frequency components through a pixel-level classification head \mathcal{C}_3 , then we have:

$$\mathcal{P}_A = \mathcal{C}_3(\tilde{\mathcal{F}}_A), \quad (9)$$

where $\mathcal{P}_A \in \mathbb{R}^{N \times k \times h \times w}$ indicates the probability of a pixel belonging to a specific class in N different frequency bands. After that, we perform a matrix multiplication \otimes between the \mathcal{P}_A and the transpose of $\tilde{\mathcal{F}}_A$ to calculate the multi-spectral class centers $\mathcal{F}_{class} \in \mathbb{R}^{N \times k \times c}$ as follows:

$$\mathcal{F}_{class} = \mathcal{P}_A \otimes \tilde{\mathcal{F}}_A^T. \quad (10)$$

Multi-spectral class centers are expected to learn a global representation of each class from a different frequency perspective. Since the class centers of the different spectra are calculated independently, there are missing interactions between them. To address this, we first treat the multi-spectral class centers as distinct nodes, then message across each node, and finally update the features for each node. The graph node modeling process can be formulated as follows:

$$\mathcal{F}'_{class} = \mathcal{G}(\mathcal{F}_{class}), \quad (11)$$

where \mathcal{G} is a GCN layer that enhances the relationships between different spectral class centers.

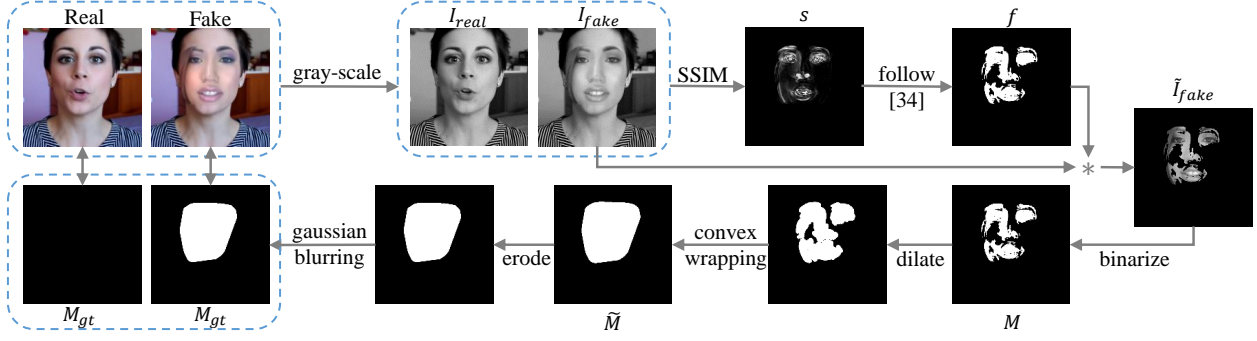


Figure 3. Pixel-level annotation procedure of FF++ [51]. The symbol $*$ is a multiplication operation.

3.3.3 Feature Refinement

We employ the multi-spectral class centers \mathcal{F}'_{class} to refine the aggregated multi-level features \mathcal{F}_A through an attentional calculation mechanism. We first compute a multi-spectral weight matrix to represent pixel similarity maps between each class center and the corresponding partial feature in \mathcal{F}_A , as follows:

$$\mathcal{W} = \text{Softmax}(\mathcal{F}_A \otimes (\mathcal{F}'_{class})^\top), \quad (12)$$

where $\mathcal{W} \in \mathbb{R}^{N \times hw \times k}$ and \mathcal{F}_A is split by channel-wise and reshaped as $N \times hw \times c$. Then, the weighted features $\mathcal{F}'_A \in \mathbb{R}^{N \times hw \times c}$ are calculated as follows:

$$\mathcal{F}'_A = \mathcal{W} \otimes \mathcal{F}'_{class}. \quad (13)$$

Finally, the multi-spectral class centers refined features $\mathcal{F}_M \in \mathbb{R}^{C \times h \times w}$ is obtained by fusing the original features \mathcal{F}_A and weighted features \mathcal{F}'_A via a *Conv* layer, we have:

$$\mathcal{F}_M = \text{Conv}(\text{Cat}([\mathcal{F}_A, \mathcal{F}'_A])). \quad (14)$$

Note that \mathcal{F}'_A is recovered and permuted to have a size of $C \times h \times w$ and the *Conv* layer to make the channel size of $2C$ to C .

Our MSCC module represents pixel-class relationships over different spectra features. The decomposed class centers are employed to calculate the attention of different frequency bands for suppressing semantic contextual information. This is because the original semantic-aware features are frequency aliasing states, with particularly low-frequency information dominating and high-frequency forgery cues easily discounted [73]. Hence, our MSCC module enhances the capacity of the model to learn semantic-agnostic features that are sensitive to face manipulation traces. In this way, the proposed MSCCNet effectively mitigates the disruption of deep semantic features in the localization decoder network, surpassing previous methods [7, 10, 22, 30, 31, 45, 61].

3.4. Objective Function

We first apply two cross-entropy loss functions for the predictions \mathcal{P}_1 and \mathcal{P}_2 of the MSCCNet, *i.e.*, a pixel-level loss \mathcal{L}_{seg} for localizing the manipulated regions and an image-level loss \mathcal{L}_{cls} for classifying the authentic or manipulated face. Then, for coarse segmentation predictions $\mathcal{P}_A \in \mathbb{R}^{N \times k \times h \times w}$ in Eq.(9), we employ a 1×1 *Conv* to fuse the multi-spectral results as follow:

$$\mathcal{P}'_A = \text{Conv}(\mathcal{P}_A), \quad (15)$$

where $\mathcal{P}'_A \in \mathbb{R}^{k \times h \times w}$ is global representations. Similarly, the cross-entropy loss function is employed to calculate its loss \mathcal{L}_{mscc} . Finally, the multi-task loss function \mathcal{L} is used to jointly optimize the model parameters, we have:

$$\mathcal{L} = \mathcal{L}_{cls} + \mathcal{L}_{seg} + \mathcal{L}_{mscc}. \quad (16)$$

4. Benchmark Datasets

To facilitate the study of face manipulation localization, we define this task as the recognition of pixel-level manipulated regions from a given face image. Since there is no single-face image dataset annotated with manipulation at pixel-level, we first construct a pixel-level single-face manipulation dataset by preprocessing and annotating the existing FF++ [51] dataset. The FF++ [51] dataset is the most widely used dataset and it provides the authentic source image corresponding to the forgery image, which establishes the theoretical support for pixel-level annotation [9, 12, 33, 61, 76]. Most previous single face forgery datasets [20, 29, 36, 69] cannot have the advantages of FF++ [51].

4.1. Pixel-level Annotation for FaceForensics++

The FF++ [51] is a challenging face forgery video dataset and consists of 1,000 original (youtube) videos and 5,000 corresponding fake videos that are generated through five typical manipulation methods, including Deepfakes (DF) [13], Face2Face (FF) [59], FaceSwap (FS)

Table 1. Details of the statistical quantity of the pixel-level FF++ [51] datasets. It includes both fake and corresponding real face images for each type of manipulation. The symbol \star denotes the removal of duplicate real face images during the validation and testing phases.

Types	Train Set	Valid Set	Test Set	All Sets
DF [13]	28,756	5,560	5,560	39,876
FF [59]	28,724	5,522	5,560	39,806
FS [17]	28,760	5,560	5,560	39,880
FSh [32]	28,760	5,560	5,560	39,880
NT [58]	28,724	5,522	5,560	39,806
All Types	143,724	16,922 \star	16,929 \star	177,575

[17], FaceShifter (FSh) [32], and NeuralTextures (NT) [58]. Meanwhile, it is adopted with three quality levels, *i.e.*, Raw Quality (C0), High Quality (C23), and Low Quality (C40).

In this paper, we further preprocess the FF++ [51] with annotations to facilitate forged region localization tasks. As shown in Figure 3, we apply the real-fake image pairs of FF++ [51] to generate the pixel-level annotation, because forgery images and their corresponding authentic images have pixel-level differences in the manipulated regions and are identical in the untampered regions [9, 12, 33, 61, 76]. To be specific, for the real face image and the fake face image of the RGB image pairs, we convert them into gray-scale (*i.e.*, I_{real} and I_{fake}) and compute the structural dissimilarity (SSIM) [63] between them to produce an SSIM map S in the range of $[0, 1]$, following [76]. To accurately portray the pixel-level discrepancy S on the forged images, we first employ the S to compute the coarse manipulated regions factor f , following [33]. Second, f and the I_{fake} are multiplied to obtain \tilde{I}_{fake} , which is then binarized to produce M . But the M still is scattered and disjointed for practical manipulation region labels, as shown in Figure 3. Therefore, we dilate the M to fill the missing tampered area and then generate a more comprehensive tamper region mask \tilde{M} by convex wrapping twice. Finally, to eliminate the deviation of the convex hull \tilde{M} edges, we apply an erosion operation to them, and then the binary manipulation mask M_{gt} is generated by Gaussian blurring followed by the threshold of 0. The above process produces the ground truth masks M_{gt} for the fake images, and for the corresponding real images, we apply zero-maps as its M_{gt} .

For each video of the FF++ [51], we interval select up to 20 frames to form the single-face manipulation image datasets and obtain the forged region labels that employ the proposed annotation procedure. Then, we divide the training, validation, and testing sets, following [51]. Finally, the detailed statistics of the pixel-level FF++ [51] as shown in Table 1.

4.2. DEFACTO

The DEFACTO [40] contains a face-swapping dataset that gathers public photo portraits on the IMDB website and selects 200 front-facing actors with a relatively neutral expression as a base to generate 3,8000 in face-swapping forgery images by an unknown method. It should be noted that this dataset retains the mask annotations of the forgery regions during the creation process, which provides us with accurate labeling, so we treat it as an unseen test set in this paper.

5. Experiments

5.1. Experimental Setup

5.1.1 Model Architecture

As previously defined, the backbone of our MSCCNet is the dilated ResNet-50 network [24], the classification branch is a simple fully connected layer, and the localization branch consists of the proposed MFA and MSCC modules. Specifically, the ResNet-50 [24] backbone is initialized by the weights pre-trained on ImageNet datasets, while the remaining layers and modules are randomly initialized. The output stride of the dilated ResNet-50 [24] is set to 8. , so $h = \frac{H}{8}$ and $w = \frac{W}{8}$ in the MSCCNet. The remaining benchmark models follow the original papers unless stated otherwise.

5.1.2 Implementation Details

We train the proposed MSCCNet with SGD setting the initial learning rate to 0.009, the momentum to 0.9, and the weight decay to $5e - 4$. The learning rate is decayed according to the “poly” learning rate policy with factor $(1 - \frac{iter}{total.iter})^{0.9}$. The size of the input images is 512×512 and the batch size is 64. We apply random horizontal flipping as the only data augmentation method for the training phase. Synchronized batch normalization implemented by Pytorch 1.8.1 is enabled during multi-GPU training. The training protocols of the remaining benchmark methods follow the original papers unless stated otherwise.

5.1.3 Benchmark Methods

We conduct a competitive benchmark for face manipulation localization, in which we train and evaluate existing forgery localization-related methods across various scenarios, including quantitative and qualitative evaluations. For the purpose of a just and reproducible comparison, we broadly select methods associated with the task of localizing tampered faces for which source code is publicly available. 1) Face manipulation detection methods with segmentation loss [7, 61]. 2) Face manipulation localization

methods [12, 45]. 3) Image forgery localization methods [10, 22, 30, 31]. These methods are described below:

HPFCN [31]: It presents a high-pass filtered fully convolutional network to locate the regions manipulated by deep inpainting. Specifically, a high-pass filter is designed to extract inpainting traces as image residuals. Then the ResNet-based fully convolutional network learns discriminative features from image residuals. However, image-level results cannot be obtained due to its lack of a classification branch.

Multi-task [45]: The work designs a multi-task learning network that includes an encoder and a Y-shaped decoder. The encoded features are used for binary classification. The output of one branch of the decoder is used for segmentation while that of the other is used for reconstruction.

FFD [12]: The method proposes to utilize an attention mechanism to process and improve the feature maps, which not only classifies the genuine or fake faces but also highlights the informative regions for manipulation localization.

M2TR [61]: The authors operate multi-scale patches to detect local inconsistencies and design a cross-modality block to fuse multi-modal forgery artifacts in the frequency and spatial domains. Additionally, the model employs extra segmentation loss to improve detection (classification) performance but does not provide pixel-level results.

SLADD [7]: The work proposes a large forgery augmentation space to enrich and strengthen types of forgeries by using the adversarial training strategy to dynamically synthesize the most challenging forgeries. The work also applies a forgery region prediction head to generate a forgery region mask, but it only aims to improve detection (classification) performance.

MVSS [10]: The method uses multi-view feature learning and multi-scale supervision to localize image manipulation regions, which exploit noise distribution information to learn semantic-agnostic features and apply boundary artifacts to address authentic images.

CATNet [30]: It focuses on JPEG compression artifacts left during image acquisition and editing, so it proposes a Compression Artifact Tracing Network that designs a convolutional neural network to learn the distribution of discrete cosine transform (DCT) coefficients. However, the DCT coefficients of image compression are not suitable for addressing video compression of FF++ [51] (*i.e.*, H.264).

HiFi-Net [22]: The authors leverage color and frequency blocks to exploit image generation artifacts that can exist in both RGB and frequency domain, then they propose a multi-branch features extractor that learns feature maps of different resolutions for the image forgery detection and localization.

Among them, M2TR [61] and SLADD [7] are only designed for Deepfake detection tasks, but we additionally compute their pixel-level results in the training and testing

phases. In the case of HPFCN [31] and MVSS [10], the output from the backbone network is utilized as input for an additional classification (detection) branch, in accordance with the network structure proposed by MSCCNet.

5.1.4 Metrics

The Accuracy (ACC) and Area Under the Receiver Operating Characteristic Curve (AUC) are reported for face manipulation detection comparison metrics, following [7, 12, 45, 61].

For the evaluation of localization results, we employ the pixel-level F1-score and mIoU (mean of class-wise intersection over union), following image forgery localization tasks [10, 22, 30, 31, 66] and semantic segmentation tasks [8, 27, 67, 74]. The higher value indicates that the performance is better.

5.2. Benchmark for Pixel-level FF++

To completely evaluate our MSCCNet, we adopt three evaluation protocols: 1) Intra-dataset: We adopt the High Quality (C23) and Low Quality (C40) of the pixel-level FF++ [51] for intra-test evaluation. 2) Unseen datasets (cross-dataset): We train the proposed method on FF++ [51] C40 dataset and then test it on unseen face-swapping datasets of DEFACTO [40]. 3) Unseen manipulations (cross-manipulation): We perform experiments on the C40 set of the pixel-level FF++ [51] dataset through a leave-one-out strategy. Specifically, there are five manipulation types of fake face images in pixel-level FF++ [51], one type is used as a test set while the remaining four types form the training set.

5.2.1 Intra-dataset Evaluation

We first investigate the localization performance of benchmark approaches on the C40 and C23 sets [51]. This task is more practical and challenging, yet is rarely explored in the previous literature. As shown in Table 2, the FFD [12] model exhibits inadequate localization results due to its utilization of low-resolution attention maps as prediction masks. Furthermore, it lacks the ability to incorporate global contextual representation in its localization branch, rendering it unsuitable for forgery localization tasks. M2TR [61] and SLADD [7] apply the semantic segmentation pipeline to supervise the manipulated regions but their main objective is to enhance detection performance rather than localization, consequently leading to unsatisfactory localization performance. Another crucial factor is the disregard for the negative impact of semantic objective information in these methods [7, 12, 45, 61]. In the image forgery localization community, while some approaches [10, 22, 30, 31] address this drawback and achieve notable

Table 2. Intra-dataset results for face manipulation localization and detection on the FF++ [51] datasets. The C40 and C23 indicate different compression levels.

Methods	References	C40				C23			
		Image-level		Pixel-level		Image-level		Pixel-level	
		ACC	AUC	F1	mIoU	ACC	AUC	F1	mIoU
HPFCN [31]	ICCV 2019	82.05	69.08	60.53	48.37	86.60	88.69	69.12	55.91
Muilt-task [45]	BTAS 2019	71.09	74.05	74.91	61.86	88.08	93.41	81.88	70.39
FFD [12]	CVPR 2020	81.65	80.05	61.24	48.84	90.94	94.54	72.63	59.27
M2TR [61]	ICMR 2022	86.18	86.34	75.33	62.02	93.44	97.18	85.13	74.78
SLADD [7]	CVPR 2022	86.25	85.53	70.95	57.86	91.12	97.23	79.96	67.87
MVSS [10]	TPAMI 2022	85.08	81.99	82.34	70.82	95.30	98.71	88.79	80.20
CAT-Net [30]	IJCV 2022	85.86	85.77	84.89	74.40	96.14	98.83	89.18	80.86
HiFi-Net [22]	CVPR 2023	72.77	80.28	76.66	63.17	89.46	97.35	84.81	74.28
MSCCNet (ours)	–	88.07	87.61	86.82	77.22	97.21	98.94	90.71	83.29

performance improvements from a noise or frequency perspective, they still struggle to effectively suppress semantic objective information in the deep features of the localization branch. For example, HPFCN [31] employs a filter on the input RGB image and only achieves a 60.53 F1-score. MVSS [10], CAT-Net [30], and HiFi-Net [22] fuse the features of the RGB image with noise- or frequency-view patterns, but they also extract them on the inputs. Hence, their localization performance on face manipulation datasets is poorer than our MSCCNet, especially on the FF++ C40 dataset [51]. This is inherently caused by the diminished discrepancy between tampered and real areas in low-quality forged images, leading to a reduction in distinctive semantic objective features and consequent localization failures. In comparison to alternative models, our MSCCNet model exhibits superior performance, especially on the C40 dataset. This outcome suggests that the proposed MFA and MSCC modules enhance global contextual representations that are semantic-agnostic features while enabling the suppression of objective semantic-related information.

We next analyze the image-level classification performance of the face forgery localization approaches on the FF++ datasets [51]. Face manipulation detection methodologies [7, 61] have already extensively studied classification tasks, so they achieve remarkable results. As shown in Table 2, these classification results of C40 sets show that FFD [12] and Multi-task [45] are not suitable for low-quality datasets. Our findings from Table 2 illustrate that preceding image forgery localization methods [22, 31] have yielded inadequate classification outcomes on the C40 and C23 datasets. Our MSCCNet outperforms all benchmark methods in terms of ACC and AUC on the C40 dataset. It is worth noting that the proposed MFA and MSCC modules are specifically designed to enhance the localization

Table 3. Generalization to unseen datasets. The model is trained on the training set of pixel-level FF++ C40 [51] datasets while tested on the face-swapping datasets of DEFACTO [40]. The * indicates an outlier as the test data is extremely unbalanced in terms of real and fake samples.

Methods	Image-level		Pixel-level	
	ACC	AUC	F1	mIoU
HPFCN [31]	60.35	48.20	59.74	47.87
Muilt-task [45]	5.82*	52.36	42.34	36.59
FFD [12]	17.54	62.03	43.68	37.31
M2TR [61]	75.82	53.16	69.90	56.93
SLADD [7]	99.36*	47.79	64.93	52.46
MVSS [10]	99.49*	50.23	59.48	42.37
CAT-Net [30]	61.90	46.45	74.07	61.04
HiFi-Net [22]	70.81	54.26	76.38	62.34
MSCCNet (ours)	85.55	64.18	77.96	65.26

branch’s function, without directly augmenting image-level classification abilities.

5.2.2 Unseen Datasets Evaluation

The unseen datasets are created by anonymous forgery methodology based on unknown source data. As shown in Table 3, we conduct cross-dataset experiments to evaluate the generalization capacity of the face manipulation localization models on unseen DEFACTO [40] datasets. Due to the highly imbalanced DEFACTO [40] dataset with a ratio of 200 real samples to 38,000 fake samples, certain methods [7, 10, 45] have encountered outliers in terms of image-level ACC. Specifically, these methods tend to predict either all real (*i.e.*, MuIt-task [45]) or all fake (*i.e.*, SLADD [7])

Table 4. Generalization to unseen manipulations on the FF++ C40 [51] dataset, which consists of five manipulation methods. We train on four methods and test on the other one method. The italicized numbers indicate the average of the five different generalization results. The F1 and mIoU in the upper table are pixel-level results, while the ACC and AUC in the lower table are image-level results.

Methods	Deepfakes		Face2Face		FaceSwap		FaceShifter		NeuralTextures		<i>Average</i>	
	F1	mIoU	F1	mIoU	F1	mIoU	F1	mIoU	F1	mIoU	<i>F1</i>	<i>mIoU</i>
HPFCN [31]	66.09	55.78	56.79	47.06	63.47	53.69	57.16	46.61	53.31	44.54	<i>59.53</i>	<i>49.54</i>
Multi-task [45]	72.74	61.17	60.77	50.04	57.25	48.54	58.21	47.75	53.42	44.88	<i>60.48</i>	<i>50.48</i>
FFD [12]	67.77	56.54	46.24	41.06	53.24	47.50	61.31	49.69	54.50	45.13	<i>56.61</i>	<i>47.98</i>
M2TR [61]	73.15	60.83	62.73	51.17	64.21	52.89	54.02	44.91	57.58	47.11	<i>62.34</i>	<i>51.38</i>
SLADD [7]	74.79	63.58	59.91	49.31	63.08	53.71	58.82	48.11	55.80	46.12	<i>62.48</i>	<i>52.17</i>
MVSS [10]	70.61	58.11	62.07	50.71	63.52	53.03	62.55	49.75	55.36	45.61	<i>62.82</i>	<i>51.44</i>
CAT-Net [30]	71.13	58.32	63.92	51.51	64.55	53.07	63.76	51.40	56.89	47.19	<i>64.05</i>	<i>52.30</i>
HiFi-Net [22]	52.41	44.94	61.35	50.15	60.74	49.83	52.64	44.12	55.26	45.97	<i>56.48</i>	<i>47.00</i>
MSCCNet (ours)	75.28	63.20	64.23	52.21	65.15	54.03	63.81	51.58	57.79	47.37	65.25	53.68

Methods	Deepfakes		Face2Face		FaceSwap		FaceShifter		NeuralTextures		<i>Average</i>	
	ACC	AUC	ACC	AUC	ACC	AUC	ACC	AUC	ACC	AUC	<i>ACC</i>	<i>AUC</i>
HPFCN [31]	58.88	68.52	55.63	57.80	53.97	55.12	58.31	61.55	54.95	57.62	<i>56.35</i>	<i>60.12</i>
Multi-task [45]	66.35	73.32	56.22	59.12	50.05	53.40	57.57	63.77	55.86	58.60	<i>57.21</i>	<i>61.64</i>
FFD [12]	65.76	71.90	63.20	68.27	53.51	56.63	58.53	63.89	56.37	59.25	<i>59.47</i>	<i>63.99</i>
M2TR [61]	66.13	75.38	61.06	65.86	56.73	60.03	57.01	61.65	57.07	60.83	<i>59.59</i>	<i>64.75</i>
SLADD [7]	63.81	75.14	61.78	65.84	59.69	63.84	60.20	65.03	57.09	59.69	<i>60.51</i>	<i>65.91</i>
MVSS [10]	69.33	77.33	59.23	63.14	58.38	62.83	58.71	62.56	55.18	58.86	<i>55.18</i>	<i>64.94</i>
CAT-Net [30]	68.09	74.86	60.61	64.26	58.65	61.74	59.37	64.27	58.38	63.53	<i>61.02</i>	<i>65.73</i>
HiFi-Net [22]	59.46	72.48	57.41	67.00	50.04	53.79	57.16	63.62	57.59	61.01	<i>56.33</i>	<i>63.58</i>
MSCCNet(ours)	69.66	80.50	61.98	67.83	60.13	63.75	60.16	64.73	58.44	62.45	62.07	67.85

and MVSS [10]) due to the extreme class imbalance. The AUC metric is calculated without considering the specific classes within the dataset. Therefore, our method demonstrates significantly better performance in terms of image-level AUC, providing strong evidence of its superiority.

Regarding the localization results for face manipulation, CAT-Net [30] and HiFi-Net [22] accomplish significant performance by learning semantic-agnostic features. However, their localization branch networks do not fully excel in this aspect. Existing forgery localization benchmark methods have not fully taken into account the semantic-agnostic features of the localization branch network. In contrast, the proposed MSCCNet effectively inhibits the image semantic content of deeper features by utilizing multi-spectral class centers, thereby achieving this target. From Table 3, our MSCCNet significantly outperforms all the competitors, which suggests that semantic-agnostic forgery cues offer a significant contribution to generalization.

5.2.3 Unseen Manipulation Evaluation

In order to assess the cross-manipulation generalization capabilities of different face manipulation localization mod-

els, we conduct the unseen manipulation evaluation experiments in Table 4. These results demonstrate that our MSCCNet achieves exceptional localization generalization performance (65.25% F1 score and 53.68% mIoU) to novel forgeries, surpassing most approaches. Despite the various manipulation methods employed in the five types of manipulations (Deepfakes [13], Face2Face [59], FaceSwap [17], FaceShifter [32], and NeuralTextures [58]) within the pixel-level FF++ dataset, each of which focuses on different tasks, the proposed MSCCNet succeeded in learning a generalized discriminative feature on four of the manipulations and generalized to the remaining one. Different types of forgeries exhibit varying levels of difficulty, with Deepfakes [13] generally being easier to detect and localize compared to NeuralTextures [58] forgeries, which are often more challenging. Furthermore, it is worth noting that the majority of face manipulation detection methods tend to have better performance in detection rather than localization, suggesting that they are primarily designed for detection tasks. Our MSCCNet also offers comparable generalizable detection results with other benchmark methods in Table 4.

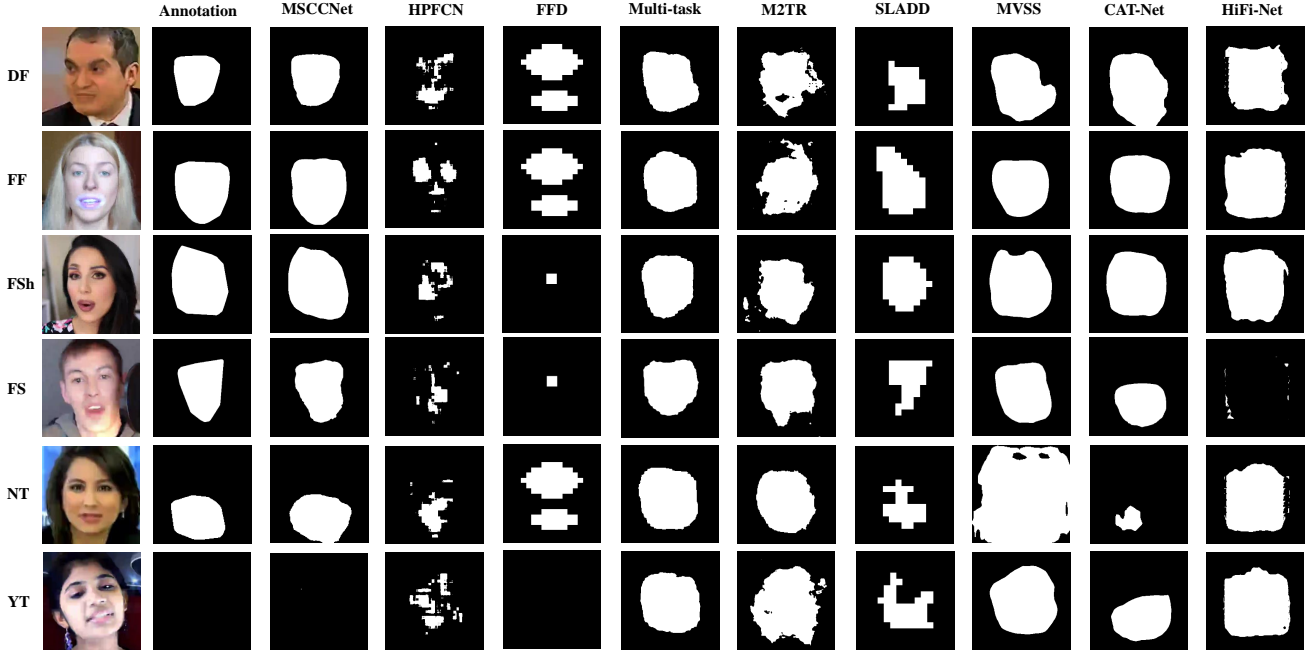


Figure 4. Visualization mask predictions of benchmark methods and our MSCCNet. The examples are randomly selected from the C40 test set of FF++ [51]. DF [13], FF [59], FSh [32], FS [17], and NT [58] rows are five different face manipulation technologies. The YT (YouTube) row is the original face image. Column Annotation indicates the proposed pixel-level manipulation region mask in this paper.

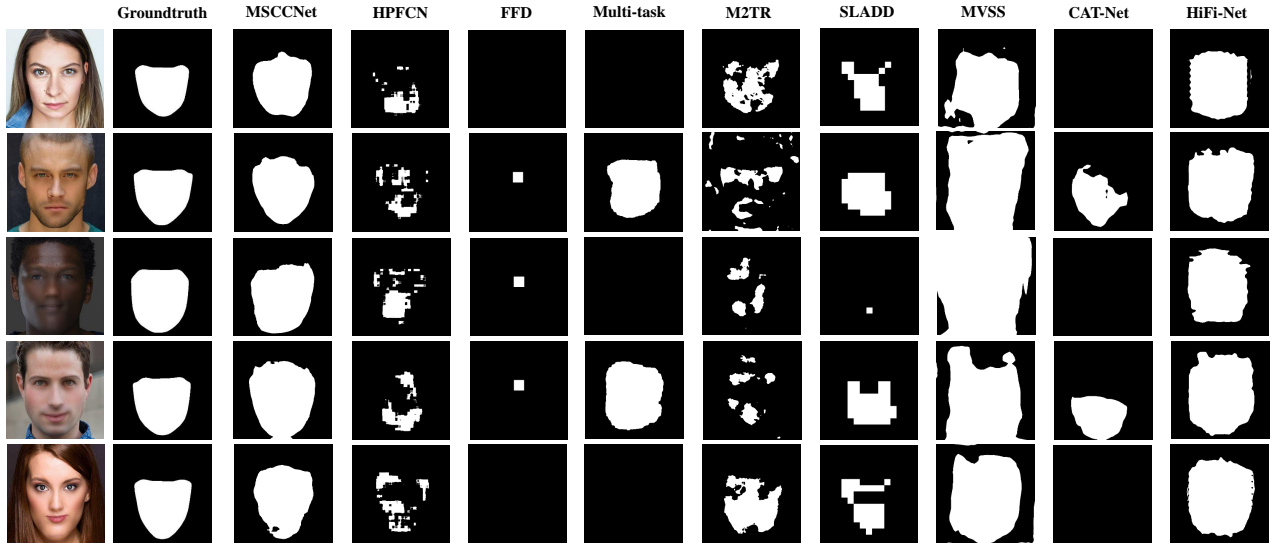


Figure 5. Generalization visualization of benchmark methods and our MSCCNet. The examples are randomly selected from the unseen DEFACTO [40] datasets. The Groundtruth columns are genuine tampered regions preserved during the data manipulation process.

5.2.4 Qualitative Comparisons

After training, our model can generate high-quality mask predictions that depict tampering locations on the test set. Here, we provide some qualitative samples in Figure 4. The predictions of FFD [12] suffer from being small and coarse due to the limited resolution of the attention map. Simi-

lar issues arise with SLADD [7], which also relies on low-resolution feature maps. HPFCN [31] proves inadequate for advanced face manipulation images, thus failing to accurately predict tampered regions. The detrimental effects of Multi-task [45] and M2TR [61], which excessively prioritize objective semantic features, are clearly evident in Figure 4. For example, NT [58] is local forgery technology,

Table 5. Extend experiment on image forgery datasets. The model is trained on the CASIAv2 [15] dataset while tested on the CASIAv1 [14] and COVER [64] datasets. The default decision threshold of 0.5 is used for all models, following MVSS [10].

Methods	Pixel-level F1		Image-level AUC	
	CASIAv1	COVER	CASIAv1	COVER
ManTra-Net [66]	15.5	28.6	14.1	54.3
CR-CNN [68]	40.5	29.1	76.6	54.6
GSR-Net [78]	38.7	28.5	50.2	45.6
MVSS [10]	45.2	45.3	83.9	57.3
MSCCNet(ours)	49.6	49.2	85.8	58.6

while Multi-task [45] and M2TR [61] predict the whole face object regions. In the case of real face images (YT row), where the facial area is the meaningless object, MVSS [10], CAT-Net [30], and HiFi-Net [22] exhibit localization errors. The superior performance of our MSCCNet is evident from its ability to identify tampered regions in distinct types of forgeries, as well as real facial images. This capability highlights the strength of our method in effectively modeling semantic-agnostic features.

In Figure 5, we present the visualization of the unseen DEFACTO [40] datasets. The results indicate that HiFi-Net [22] demonstrates superior generalization performance compared to other benchmark methods, although it falls short in capturing fine edge details. However, thanks to the integration of the MFA module and MSCC module in our method, we achieve more accurate predictions of details and demonstrate enhanced generalization capabilities.

5.3. Extend Experiment

To further validate the effectiveness of our approach, we conducted experiments on the image forgery datasets following the experiment setting of the MVSS [10]. In general, the training dataset consists of CASIAv2 [15], which contains 7,491 real samples and 5,063 fake samples, including both copy-move and splitting image editing types. There are two unseen testing datasets used for evaluation. The first dataset, CASIAv1 [14], comprises 800 images and 920 fake images, including both copy-move and splitting image editing types. The second dataset, COVER [64], consists of 100 samples and 100 copy-move manipulated samples.

As presented in Table 5, the localization and detection results for other comparisons are obtained from the original MVSS paper [10]. Based on the results, it is evident that our MSCCNet outperforms other methods in terms of pixel-level F1-score. Additionally, it achieves comparable image-level performance with the best-performing MVSS method [10]. These indicate that our method learns generalizable forgery features for transferability across different manipulation datasets.

Table 6. Analysis of different modules of the proposed MSCCNet.

Base.	MFA	MSCC	\mathcal{L}_{mscc}	Image-level		Pixel-level	
				ACC	AUC	F1	mIoU
✓	-	-	-	87.49	86.67	83.79	72.84
✓	✓	-	-	87.29	86.68	83.98	73.11
✓	✓	✓	-	87.38	86.99	85.82	75.76
✓	✓	✓	✓	88.07	87.61	86.82	77.22

5.4. Ablation Study

We analyze different modules of proposed MSCCNet on the FF++ [51] C40 dataset and adopt the intra-dataset evaluation protocol.

5.4.1 Analysis on MSCCNet Architecture

We set the baseline (*Base.*) model by removing the MFA and MSCC modules, and the remaining convolutional blocks. As summarized in Table 6, applying the MFA module could bring 0.27% mIoU improvements, which demonstrates that low-level local textures are helpful for manipulated region localization. MSCC module is the key component for modeling semantic-agnostic features, it achieves 75.76% in terms of mIoU. The multi-spectral features of the coarse segmentation supervision mechanism enable the assessment of the probability of pixel attribution to its specific class. These features subsequently drive the MSCC module’s ability to approximate a robust class center. From the last line in Table 6, we can observe that \mathcal{L}_{mscc} improves the localization performance from 75.76% to 77.22%. Our results show that the combination of semantic-agnostic features and low-level artifacts improves face manipulation localization. Moreover, the proposed MSCC module offers a viable solution to suppress semantic-related information through a multi-frequency perspective.

5.4.2 Influence of GCN

The GCN layer in our MSCC module improves the consistency of multi-spectral class-level representations by enhancing interaction between class centers across various frequency bands. As can be seen in Table 7, if the GCN layer is removed, the localization performance drops from 77.22% to 76.62% mIoU. It helps with multi-frequency attention map calculation in feature refinement operations.

5.4.3 Influence of DCT Filters

In Sec. 3.3, the DCT filters decompose semantic context features to different frequency bands, which relieves the aliasing among low-frequency and high-frequency components [73]. Given that forgery traces are more prominent in high-frequency rather than low-frequency compo-

Table 7. Analysis of the proposed MSCC module.

GCN	DCT	Add	Concat	Image-level		Pixel-level	
				ACC	AUC	F1	mIoU
✓	✓	-	✓	88.07	87.61	86.82	77.22
-	✓	-	✓	87.60	87.17	86.41	76.62
✓	-	-	✓	87.61	87.43	85.94	75.92
✓	✓	✓	-	88.03	87.10	86.44	76.66

Table 8. Analysis of the number of transformation basis of the MSCC module.

Number of Transformation Basis	Image-level		Pixel-level	
	ACC	AUC	F1	mIoU
1	87.68	86.83	86.23	76.34
4	88.07	87.61	86.82	77.22
16	88.06	87.44	86.46	76.70

nents [9, 37, 39, 48, 61], the multi-spectral class centers have the potential to model frequency-dependent forgery traces, particularly in high-frequency regions. To show the effectiveness, we remove the DCT filters of the MSCC module, the performance drops to 75.92%. In comparison, applying DCT filters brings 1.3% mIoU improvements, as indicated in Table 7.

5.4.4 Influence of Fusion Type

There are two feature fusion types: addition (Add) and concatenation (Concat) options for Eq. (14). In Table 7, we try both addition and concatenation, and the experimental results demonstrate that the concatenation type is better performance.

5.4.5 Influence of the Number of Transformation Basis

The number of transformation basis of 2D DCT can be denoted as N in Sec. 3.3. To investigate the performance of using different N , various experiments are conducted and the experimental results are shown in Table 8. When setting N to 1, the (u, v) only is $(0, 0)$, which indicates that the features are decomposed to low-frequency components and miss high-frequency forgery traces. Thus, its mIoU is 0.88% lower than $N = 4$. Note that $N = 4$ means the (u, v) is $(0, 0)$, $(0, 1)$, $(1, 0)$, and $(1, 1)$, which decomposes the more frequency components including low- and high-frequency. We also notice that performance drops to 76.70 if we use $N = 16$. This is primarily due to the increased difficulty of predicting accurate coarse segmentation outcomes for multi-frequency features, resulting in inadequate class-level representations when N is too large. Therefore, we adopt $N = 4$ for the other experiments.

6. Discussion and Conclusion

This paper proposes a novel Multi-spectral Class Centers Network (MSCCNet) to facilitate the acquisition of more generalizable and semantic-agnostic features for improved face manipulation localization outcomes. To avoid reliance on semantic objective information, we employ the multi-spectral class centers (MSCC) module to compute different frequency class-level contexts and weighted attention, which enables the refinement of deep semantic features. The Multi-level Feature Aggregation (MFA) module is integrated to fuse low-level forgery-specific textures. Our extensive experiments demonstrate the superior localization ability of MSCCNet on comprehensive benchmarks introduced in this paper.

However, we remain cognizant of certain limitations that exist in this paper. First, it must be acknowledged that the pixel-level annotation method proposed in this work may not generate absolute and unequivocal tampering mask labels. Nevertheless, none of the current existing single-face manipulation datasets offer definitive and ground-truth tampering mask labels. This makes the masks generated based on pixel-level disparities between real-fake-image pairs the most suitable approximation of the ground-truth labels. Our approach and benchmark can be readily utilized in the event that more precisely-formed forged region mask labels come to fruition. Besides, the proposed MSCCNet makes no attempt to improve classification performance, since recent methodologies for single-face classification have been extensively studied. Moving forward, we plan to investigate and optimize both the classification and location branches of our approach in a unified fashion.

References

- [1] Darius Afchar, Vincent Nozick, Junichi Yamagishi, and Isao Echizen. Mesonet: a compact facial video forgery detection network. In *2018 IEEE International Workshop on Information Forensics and Security (WIFS)*, pages 1–7. IEEE, 2018. 3
- [2] Nasir Ahmed, T. Natarajan, and Kamisetty R Rao. Discrete cosine transform. *IEEE transactions on Computers*, 100(1):90–93, 1974. 5
- [3] Jawadul H. Bappy, Amit K. Roy-Chowdhury, Jason Bunk, Lakshmanan Nataraj, and B. S. Manjunath. Exploiting spatial structure for localizing manipulated image regions. *2017 IEEE International Conference on Computer Vision (ICCV)*, pages 4980–4989, 2017. 2, 3, 4
- [4] Belhassen Bayar and Matthew C Stamm. A deep learning approach to universal image manipulation detection using a new convolutional layer. In *Proceedings of the 4th ACM Workshop on Information Hiding and Multimedia Security*, pages 5–10, 2016. 2
- [5] Belhassen Bayar and Matthew C Stamm. Constrained convolutional neural networks: A new approach towards general purpose image manipulation detection. *IEEE Transactions*

- on *Information Forensics and Security*, 13(11):2691–2706, 2018. 3
- [6] Tiago Carvalho, Fabio A Faria, Helio Pedrini, Ricardo da S Torres, and Anderson Rocha. Illuminant-based transformed spaces for image forensics. *IEEE transactions on information forensics and security*, 11(4):720–733, 2015. 3
- [7] Liang Chen, Yong Zhang, Yibing Song, Lingqiao Liu, and Jue Wang. Self-supervised learning of adversarial example: Towards good generalizations for deepfake detection. In *Proceedings of the IEEE/CVF conference on computer vision and pattern recognition*, pages 18710–18719, 2022. 2, 6, 7, 8, 9, 10, 11
- [8] Liang-Chieh Chen, George Papandreou, Florian Schroff, and Hartwig Adam. Rethinking atrous convolution for semantic image segmentation. *arXiv preprint arXiv:1706.05587*, 2017. 4, 8
- [9] Shen Chen, Taiping Yao, Yang Chen, Shouhong Ding, Jilin Li, and Rongrong Ji. Local relation learning for face forgery detection. In *Proceedings of the AAAI Conference on Artificial Intelligence*, volume 35, pages 1081–1088, 2021. 2, 3, 5, 6, 7, 13
- [10] Xinru Chen, Chengbo Dong, Jiaqi Ji, Juan Cao, and Xirong Li. Image manipulation detection by multi-view multi-scale supervision. In *Proceedings of the IEEE/CVF International Conference on Computer Vision*, pages 14185–14193, 2021. 2, 3, 4, 6, 8, 9, 10, 12
- [11] Davide Cozzolino, Diego Gragnaniello, and Luisa Verdoliva. Image forgery localization through the fusion of camera-based, feature-based and pixel-based techniques. In *2014 IEEE International Conference on Image Processing (ICIP)*, pages 5302–5306. IEEE, 2014. 3
- [12] Hao Dang, Feng Liu, Joel Stehouwer, Xiaoming Liu, and Anil K Jain. On the detection of digital face manipulation. In *Proceedings of the IEEE/CVF Conference on Computer Vision and Pattern Recognition*, pages 5781–5790, 2020. 2, 3, 4, 6, 7, 8, 9, 10, 11
- [13] DeepFakes. <https://github.com/deepfakes/>, 2019. 1, 3, 6, 7, 10, 11
- [14] J. Dong, W. Wang, and T. Tan. Casia image tampering detection evaluation database. <http://forensics.idealtest.org>, 2010. 12
- [15] J. Dong, W. Wang, and T. Tan. Casia image tampering detection evaluation database. In *IEEE China summit and international conference on signal and information processing (ChinaSIP)*, pages 422–426. IEEE, 2013. 12
- [16] Ricard Durall, Margret Keuper, Franz-Josef Pfreundt, and Janis Keuper. Unmasking deepfakes with simple features. *arXiv preprint arXiv:1911.00686*, 2019. 3
- [17] FaceSwap. <https://github.com/MarekKowalski/FaceSwap>, 2019. 1, 3, 7, 10, 11
- [18] Pasquale Ferrara, Tiziano Bianchi, Alessia De Rosa, and Alessandro Piva. Image forgery localization via fine-grained analysis of cfa artifacts. *IEEE Transactions on Information Forensics and Security*, 7(5):1566–1577, 2012. 3
- [19] Jessica Fridrich and Jan Kodovsky. Rich models for steganalysis of digital images. *IEEE Transactions on Information Forensics and Security*, 7(3):868–882, 2012. 2, 3
- [20] google ai. <https://ai.googleblog.com/2019/09/contributing-data-to-deepfake-detection.html>, 2019. 6
- [21] Qiqi Gu, Shen Chen, Taiping Yao, Yang Chen, Shouhong Ding, and Ran Yi. Exploiting fine-grained face forgery clues via progressive enhancement learning. *arXiv preprint arXiv:2112.13977*, 2021. 3
- [22] Xiao Guo, Xiaohong Liu, Zhiyuan Ren, Steven Grosz, Iacopo Masi, and Xiaoming Liu. Hierarchical fine-grained image forgery detection and localization. In *Proceedings of the IEEE/CVF Conference on Computer Vision and Pattern Recognition*, pages 3155–3165, 2023. 2, 3, 4, 6, 8, 9, 10, 12
- [23] Jing Hao, Zhixin Zhang, Shicai Yang, Di Xie, and Shiliang Pu. Transforensics: Image forgery localization with dense self-attention. *2021 IEEE/CVF International Conference on Computer Vision (ICCV)*, pages 15035–15044, 2021. 2, 3, 4
- [24] Kaiming He, X. Zhang, Shaoqing Ren, and Jian Sun. Deep residual learning for image recognition. *2016 IEEE Conference on Computer Vision and Pattern Recognition (CVPR)*, pages 770–778, 2015. 7
- [25] Yihao Huang, Felix Juefei-Xu, Run Wang, Xiaofei Xie, L. Ma, Jianwen Li, Weikai Miao, Yang Liu, and Geguang Pu. Fakelocator: Robust localization of gan-based face manipulations. *IEEE Transactions on Information Forensics and Security*, 17:2657–2672, 2020. 2, 3, 4
- [26] Gengyun Jia, Meisong Zheng, Chuanrui Hu, Xin Ma, Yuting Xu, Luoqi Liu, Yafeng Deng, and Ran He. Inconsistency-aware wavelet dual-branch network for face forgery detection. *IEEE Transactions on Biometrics, Behavior, and Identity Science*, 3(3):308–319, 2021. 2, 3, 4
- [27] Alexander Kirillov, Ross B. Girshick, Kaiming He, and Piotr Dollár. Panoptic feature pyramid networks. *2019 IEEE/CVF Conference on Computer Vision and Pattern Recognition (CVPR)*, pages 6392–6401, 2019. 4, 8
- [28] Chenqi Kong, Baoliang Chen, Haoliang Li, Shiqi Wang, Anderson Rocha, and Sam Kwong. Detect and locate: Exposing face manipulation by semantic-and noise-level telltales. *IEEE Transactions on Information Forensics and Security*, 17:1741–1756, 2022. 2, 3
- [29] Pavel Korshunov and Sébastien Marcel. Deepfakes: a new threat to face recognition? assessment and detection. *arXiv preprint arXiv:1812.08685*, 2018. 6
- [30] Myung-Joon Kwon, Seung-Hun Nam, In-Jae Yu, Heung-Kyu Lee, and Changick Kim. Learning jpeg compression artifacts for image manipulation detection and localization. *International Journal of Computer Vision*, 130(8):1875–1895, 2022. 2, 3, 4, 6, 8, 9, 10, 12
- [31] Haodong Li and Ji Wu Huang. Localization of deep inpainting using high-pass fully convolutional network. In *proceedings of the IEEE/CVF international conference on computer vision*, pages 8301–8310, 2019. 2, 3, 4, 6, 8, 9, 10, 11
- [32] Lingzhi Li, Jianmin Bao, Hao Yang, Dong Chen, and Fang Wen. Faceshifter: Towards high fidelity and occlusion aware face swapping. *arXiv preprint arXiv:1912.13457*, 2019. 1, 3, 7, 10, 11
- [33] Lingzhi Li, Jianmin Bao, Ting Zhang, Hao Yang, Dong Chen, Fang Wen, and Baining Guo. Face x-ray for more general face forgery detection. In *Proceedings of the IEEE/CVF*

- Conference on Computer Vision and Pattern Recognition*, pages 5001–5010, 2020. 2, 3, 6, 7
- [34] Xiaodan Li, Yining Lang, Yuefeng Chen, Xiaofeng Mao, Yuan He, Shuhui Wang, Hui Xue, and Quan Lu. Sharp multiple instance learning for deepfake video detection. In *Proceedings of the 28th ACM international conference on multimedia*, pages 1864–1872, 2020. 2
- [35] Yuezun Li and Siwei Lyu. Exposing deepfake videos by detecting face warping artifacts. *arXiv preprint arXiv:1811.00656*, 2018. 2
- [36] Yuezun Li, Xin Yang, Pu Sun, Hongang Qi, and Siwei Lyu. Celeb-df: A large-scale challenging dataset for deepfake forensics. In *Proceedings of the IEEE/CVF Conference on Computer Vision and Pattern Recognition*, pages 3207–3216, 2020. 6
- [37] Honggu Liu, Xiaodan Li, Wenbo Zhou, Yuefeng Chen, Yuan He, Hui Xue, Weiming Zhang, and Nenghai Yu. Spatial-phase shallow learning: rethinking face forgery detection in frequency domain. In *Proceedings of the IEEE/CVF Conference on Computer Vision and Pattern Recognition*, pages 772–781, 2021. 2, 3, 4, 5, 13
- [38] Sun’ao Liu, Hongtao Xie, Hai Xu, Yongdong Zhang, and Qi Tian. Partial class activation attention for semantic segmentation. *2022 IEEE/CVF Conference on Computer Vision and Pattern Recognition (CVPR)*, pages 16815–16824, 2022. 4
- [39] Yuchen Luo, Yong Zhang, Junchi Yan, and Wei Liu. Generalizing face forgery detection with high-frequency features. In *Proceedings of the IEEE/CVF Conference on Computer Vision and Pattern Recognition*, pages 16317–16326, 2021. 2, 3, 4, 5, 13
- [40] Gaël Mahfoudi, Badr Tajini, Florent Retraint, Frederic Morain-Nicolier, Jean Luc Dugelay, and PIC Marc. Defacto: Image and face manipulation dataset. In *2019 27th european signal processing conference (EUSIPCO)*, pages 1–5. IEEE, 2019. 7, 8, 9, 11, 12
- [41] Iacopo Masi, Aditya Killekar, Royston Marian Mascarenhas, Shenoy Pratik Gurudatt, and Wael AbdAlmageed. Two-branch recurrent network for isolating deepfakes in videos. In *European Conference on Computer Vision*, pages 667–684. Springer, 2020. 3
- [42] Changtao Miao, Qi Chu, Weihai Li, Suichan Li, Zhentao Tan, Wanyi Zhuang, and Nenghai Yu. Learning forgery region-aware and id-independent features for face manipulation detection. *IEEE Transactions on Biometrics, Behavior, and Identity Science*, 4(1):71–84, 2022. 3
- [43] Changtao Miao, Zichang Tan, Qi Chu, Huan Liu, Honggang Hu, and Nenghai Yu. F 2 trans: High-frequency fine-grained transformer for face forgery detection. *IEEE Transactions on Information Forensics and Security*, 18:1039–1051, 2023. 3
- [44] Changtao Miao, Zichang Tan, Qi Chu, Nenghai Yu, and Guodong Guo. Hierarchical frequency-assisted interactive networks for face manipulation detection. *IEEE Transactions on Information Forensics and Security*, 17:3008–3021, 2022. 3
- [45] Huy H Nguyen, Fuming Fang, Junichi Yamagishi, and Isao Echizen. Multi-task learning for detecting and segmenting manipulated facial images and videos. In *2019 IEEE 10th international conference on biometrics theory, applications and systems (BTAS)*, pages 1–8. IEEE, 2019. 2, 3, 4, 6, 8, 9, 10, 11, 12
- [46] Xunyu Pan, Xing Zhang, and Siwei Lyu. Exposing image splicing with inconsistent local noise variances. In *2012 IEEE International Conference on Computational Photography (ICCP)*, pages 1–10. IEEE, 2012. 3
- [47] Bo Peng, Wei Wang, Jing Dong, and Tieniu Tan. Optimized 3d lighting environment estimation for image forgery detection. *IEEE Transactions on Information Forensics and Security*, 12(2):479–494, 2016. 3
- [48] Yuyang Qian, Guojun Yin, Lu Sheng, Zixuan Chen, and Jing Shao. Thinking in frequency: Face forgery detection by mining frequency-aware clues. In *European Conference on Computer Vision*, pages 86–103. Springer, 2020. 2, 3, 5, 13
- [49] Zequn Qin, Pengyi Zhang, Fei Wu, and Xi Li. Fcanet: Frequency channel attention networks. In *2021 IEEE/CVF International Conference on Computer Vision (ICCV)*, pages 783–792. IEEE, 2021. 5
- [50] Nicolas Rahmouni, Vincent Nozick, Junichi Yamagishi, and Isao Echizen. Distinguishing computer graphics from natural images using convolution neural networks. *2017 IEEE Workshop on Information Forensics and Security (WIFS)*, pages 1–6, 2017. 3
- [51] Andreas Rossler, Davide Cozzolino, Luisa Verdoliva, Christian Riess, Justus Thies, and Matthias Nießner. Faceforensics++: Learning to detect manipulated facial images. In *Proceedings of the IEEE International Conference on Computer Vision*, pages 1–11, 2019. 1, 2, 6, 7, 8, 9, 10, 11, 12
- [52] Evan Shelhamer, Jonathan Long, and Trevor Darrell. Fully convolutional networks for semantic segmentation. *2015 IEEE Conference on Computer Vision and Pattern Recognition (CVPR)*, pages 3431–3440, 2014. 4
- [53] Kaede Shiohara and T. Yamasaki. Detecting deepfakes with self-blended images. *2022 IEEE/CVF Conference on Computer Vision and Pattern Recognition (CVPR)*, pages 18699–18708, 2022. 2, 3
- [54] Luchuan Song, Zheng Fang, Xiaodan Li, Xiaoyi Dong, Zhenchao Jin, Yuefeng Chen, and Siwei Lyu. Adaptive face forgery detection in cross domain. In *Computer Vision—ECCV 2022: 17th European Conference, Tel Aviv, Israel, October 23–27, 2022, Proceedings, Part XXXIV*, pages 467–484. Springer, 2022. 3
- [55] Luchuan Song, Xiaodan Li, Zheng Fang, Zhenchao Jin, Yuefeng Chen, and Chenliang Xu. Face forgery detection via symmetric transformer. In *Proceedings of the 30th ACM International Conference on Multimedia*, pages 4102–4111, 2022. 3
- [56] Kritaphat Songsri-in and Stefanos Zafeiriou. Complement face forensic detection and localization with facial landmarks. *ArXiv*, abs/1910.05455, 2019. 2, 3, 4
- [57] Zichang Tan, Zhichao Yang, Changtao Miao, and Guodong Guo. Transformer-based feature compensation and aggregation for deepfake detection. *IEEE Signal Processing Letters*, 29:2183–2187, 2022. 3
- [58] Justus Thies, Michael Zollhöfer, and Matthias Nießner. Deferred neural rendering: Image synthesis using neural tex-

- tures. *ACM Transactions on Graphics (TOG)*, 38(4):1–12, 2019. 1, 2, 3, 7, 10, 11
- [59] Justus Thies, Michael Zollhofer, Marc Stamminger, Christian Theobalt, and Matthias Nießner. Face2face: Real-time face capture and reenactment of rgb videos. In *Proceedings of the IEEE conference on computer vision and pattern recognition*, pages 2387–2395, 2016. 1, 3, 6, 7, 10, 11
- [60] Chengrui Wang and Weihong Deng. Representative forgery mining for fake face detection. In *Proceedings of the IEEE/CVF Conference on Computer Vision and Pattern Recognition*, pages 14923–14932, 2021. 3
- [61] Junke Wang, Zuxuan Wu, Jingjing Chen, and Yu-Gang Jiang. M2tr: Multi-modal multi-scale transformers for deepfake detection. *arXiv preprint arXiv:2104.09770*, 2021. 2, 3, 6, 7, 8, 9, 10, 11, 12, 13
- [62] Run Wang, Felix Juefei-Xu, Lei Ma, Xiaofei Xie, Yihao Huang, Jian Wang, and Yang Liu. Fakespotter: A simple yet robust baseline for spotting ai-synthesized fake faces. In *International Joint Conference on Artificial Intelligence (IJCAI)*, 2020. 3
- [63] Zhou Wang, Alan Conrad Bovik, Hamid R. Sheikh, and Eero P. Simoncelli. Image quality assessment: from error visibility to structural similarity. *IEEE Transactions on Image Processing*, 13:600–612, 2004. 7
- [64] B. Wen, Y. Zhu, R. Subramanian, T. T. Ng, and S. Winkler. Coverage-a novel database for copy-move forgery detection. In *IEEE international conference on image processing (ICIP)*, pages 161–165. IEEE, 2016. 12
- [65] Haiwei Wu, Jiantao Zhou, Shile Zhang, and Jinyu Tian. Exploring spatial-temporal features for deepfake detection and localization. *ArXiv*, abs/2210.15872, 2022. 2, 3, 4
- [66] Yue Wu, Wael AbdAlmageed, and P. Natarajan. Mantra-net: Manipulation tracing network for detection and localization of image forgeries with anomalous features. *2019 IEEE/CVF Conference on Computer Vision and Pattern Recognition (CVPR)*, pages 9535–9544, 2019. 2, 3, 4, 8, 12
- [67] Tete Xiao, Yingcheng Liu, Bolei Zhou, Yuning Jiang, and Jian Sun. Unified perceptual parsing for scene understanding. *ArXiv*, abs/1807.10221, 2018. 4, 8
- [68] Chao Yang, Huizhou Li, Fangting Lin, Bin Jiang, and Hao Zhao. Constrained r-cnn: A general image manipulation detection model. In *2020 IEEE International conference on multimedia and expo (ICME)*, pages 1–6. IEEE, 2020. 12
- [69] Xin Yang, Yuezun Li, and Siwei Lyu. Exposing deep fakes using inconsistent head poses. In *ICASSP 2019-2019 IEEE International Conference on Acoustics, Speech and Signal Processing (ICASSP)*, pages 8261–8265. IEEE, 2019. 2, 6
- [70] Peipeng Yu, Jianwei Fei, Zhihua Xia, Zhili Zhou, and Jian Weng. Improving generalization by commonality learning in face forgery detection. *IEEE Transactions on Information Forensics and Security*, 17:547–558, 2022. 2, 3
- [71] Yuhui Yuan, Xilin Chen, and Jingdong Wang. Object-contextual representations for semantic segmentation. *ArXiv*, abs/1909.11065, 2019. 4
- [72] Fan Zhang, Yanqin Chen, Zhihang Li, Zhibin Hong, Jingtuo Liu, Feifei Ma, Junyu Han, and Errui Ding. Acfnnet: Attentional class feature network for semantic segmentation. *2019 IEEE/CVF International Conference on Computer Vision (ICCV)*, pages 6797–6806, 2019. 4
- [73] Richard Zhang. Making convolutional networks shift-invariant again. In *International conference on machine learning*, pages 7324–7334. PMLR, 2019. 6, 12
- [74] Hengshuang Zhao, Jianping Shi, Xiaojuan Qi, Xiaogang Wang, and Jiaya Jia. Pyramid scene parsing network. *2017 IEEE Conference on Computer Vision and Pattern Recognition (CVPR)*, pages 6230–6239, 2016. 4, 8
- [75] Hanqing Zhao, Wenbo Zhou, Dongdong Chen, Tianyi Wei, Weiming Zhang, and Nenghai Yu. Multi-attentional deepfake detection. In *Proceedings of the IEEE/CVF Conference on Computer Vision and Pattern Recognition*, pages 2185–2194, 2021. 2, 3
- [76] Tianchen Zhao, Xiang Xu, Mingze Xu, Hui Ding, Yuanjun Xiong, and Wei Xia. Learning self-consistency for deepfake detection. In *Proceedings of the IEEE/CVF International Conference on Computer Vision (ICCV)*, pages 15023–15033, October 2021. 2, 3, 6, 7
- [77] Peng Zhou, Bor-Chun Chen, Xintong Han, Mahyar Najibi, and Larry S. Davis. Generate, segment and replace: Towards generic manipulation segmentation. In *AAAI Conference on Artificial Intelligence*, 2018. 2, 3, 4
- [78] Peng Zhou, Bor-Chun Chen, Xintong Han, Mahyar Najibi, Abhinav Shrivastava, Ser-Nam Lim, and Larry Davis. Generate, segment, and refine: Towards generic manipulation segmentation. In *Proceedings of the AAAI conference on artificial intelligence*, volume 34, pages 13058–13065, 2020. 12
- [79] Wanyi Zhuang, Qi Chu, Zhentao Tan, Qiankun Liu, Haojie Yuan, Changtao Miao, Zixiang Luo, and Nenghai Yu. Uia-vit: Unsupervised inconsistency-aware method based on vision transformer for face forgery detection. In *Computer Vision—ECCV 2022: 17th European Conference, Tel Aviv, Israel, October 23–27, 2022, Proceedings, Part V*, pages 391–407. Springer, 2022. 3
- [80] Wanyi Zhuang, Qi Chu, Haojie Yuan, Changtao Miao, Bin Liu, and Nenghai Yu. Towards intrinsic common discriminative features learning for face forgery detection using adversarial learning. In *2022 IEEE International Conference on Multimedia and Expo (ICME)*, pages 1–6. IEEE, 2022. 3